

Cambridge Centre for Computational Chemical Engineering

University of Cambridge

Department of Chemical Engineering

Preprint

ISSN 1473 – 4273

Sources of emissions of CO and the Effects of Varying the Octane Number in an HCCI Engine

Amit Bhave, Markus Kraft,¹ Luca Montorsi,² Fabian Mauss³

submitted: 20th September 2005

¹ Department of Chemical Engineering
University of Cambridge
Pembroke Street
Cambridge CB2 3RA
UK
E-Mail: markus_kraft@cheng.cam.ac.uk

² Department of Mechanical Engineering
University of Modena and Reggio Emilia
Via Vignolese, 905/a, Modena
Italy

³ Division of Combustion Physics
Lund Institute of Technology
Box 118, S-221 00 Lund
Sweden

Preprint No. 18



c4e

Key words and phrases. HCCI, CO emissions, octane number.

Edited by

Cambridge Centre for Computational Chemical Engineering
Department of Chemical Engineering
University of Cambridge
Cambridge CB2 3RA
United Kingdom.

Fax: + 44 (0)1223 334796

E-Mail: c4e@cheng.cam.ac.uk

World Wide Web: <http://www.cheng.cam.ac.uk/c4e/>

Abstract

We investigate the factors which influence a reliable prediction of CO emissions in a dual-fuelled, homogeneous charge compression ignition (HCCI) engine using an improved probability density function (PDF) based engine cycle model. A convective heat loss sub-model (based on a stochastic jump process) and a coalescence-dispersion approach have been included to account for inhomogeneities due to fluctuations, turbulent mixing and fluid-wall interactions. A base case comparison of the model predictions with the measurements (Olsson et al. SAE paper 2000-01-2867) suggests a good agreement between the model calculations and experimental results for auto-ignition timing, peak pressure as well as CO, HC and NO_x emissions. Based on the model, fluid-wall interactions, mixing of the hot and cold fluid parcels, and cylinder wall temperature have been identified to be critical for correctly predicting CO emissions, a task inherently difficult for the existing HCCI models in the literature. Furthermore, the role of octane number in controlling (HCCI) combustion and emissions is investigated and the model predictions are compared with measurements. The auto-ignition timing and the in-cylinder pressure and emissions are observed to be sensitive to the variation in octane number. The magnitudes as well as the trends for the combustion parameters and the emissions (CO, HC and NO_x) with respect to octane number are predicted reasonably well by the model.

Contents

1	Introduction	3
2	Engine description	5
3	Model description	6
4	Model validation	8
5	CO emissions	12
6	Wall temperature sensitivity	15
7	In-cylinder temperature distribution	16
8	Octane number variation	18
9	Conclusions	21
10	Acknowledgements	21
	References	21

1 Introduction

Evident environmental and efficiency benefits have provided the impetus for research and advancement of homogeneous charge compression ignition (HCCI) technology. In particular, modelling efforts have been triggered by improvements in processing and storage power. With its advantages of including residual burnt fraction, modelling gas exchange processes and accounting for the exact temperature at inlet valve closure (IVC), engine cycle models have replaced the old closed-volume approach of modelling compression, ignition and expansion strokes only. Single zone, multi-zone, CFD coupled and CFD driven full cycle HCCI models have been reported in the literature. As compared to the single zone models, the multi-zone and CFD based models have improved the predictions of in-cylinder pressure and emissions at the expense of higher computational time.

The single zone, multi-zone and CFD based models developed for HCCI, however, generally predict CO emissions poorly (Flowers et al.; 2002). The poor prediction of CO emissions using a single zone engine cycle model can be attributed to its inability in accounting for the inhomogeneities in temperature and composition. A closed volume 10-zone model applied to study natural gas fuelled HCCI combustion faced intrinsic difficulty in predicting the CO emissions, under-predicting the measurements by an order of magnitude (Aceves et al.; 2000). Following that, the sequential multi-zone model (Aceves et al.; 2001a) and the segregated solver (CFD-driven) (Aceves et al.; 2001b) approaches also showed an error of around 70% in predicting the experimental results for CO emissions. Easley et al. (2001) attributed such under-prediction to the lack of mass and energy transfer between the zones and emphasized the need for a more detailed description of the in-cylinder temperature distribution. A 9-zone based full cycle model with mass exchange between zones has been applied for gasoline HCCI modelling (Ogink and Golovitchev; 2002). However, to obtain a good agreement between CO predictions and experimental results, the rate constant for the CO oxidation reaction was adjusted assuming that it does not violate the auto-ignition characteristics of the mechanism. A CFD-coupled engine cycle model has been used to investigate iso-octane HCCI combustion (Kong and Reitz; 2003). This KIVA-3V based model with the eddy break up concept, located the cylinder liner wall as a major source of CO emissions. However, the CO emissions were under-predicted by 80%. In the same study, the sensitivity of the rate constant for the CO oxidation reaction on the CO predictions was observed to be high. Ogink and Golovitchev (2002) have pointed out that implementing a certain inhomogeneity in the perfectly-stirred individual zones of the multi-zone model could improve the prediction of CO emissions.

Probability density function (PDF) based models can account for such inhomogeneities. The closed volume PDF-based stochastic reactor model (SRM) has been demonstrated to correctly predict the ignition timing, in-cylinder pressure and emissions in an HCCI engine (Kraft et al.; 2000; Maigaard et al.; 2003). However this modelling approach involved splitting the in-cylinder mass into a rigid boundary layer (20%) and a bulk zone (80%), with a deterministic convective heat loss sub-

model. Thus the model did not account for the changing in-cylinder mass in the boundary layer (Fiveland and Assanis; 2001). Also, the local temperature inhomogeneity attributed to the thermal boundary layer was lost during mixing. To overcome these drawbacks, an improved SRM with a convective heat loss sub-model based on Woschni's coefficient and a stochastic jump process, has been introduced and demonstrated to have reliably predicted the effect of exhaust gas recirculation (EGR) on natural gas fuelled HCCI combustion and emissions (Bhave et al.; 2004). The improved PDF-based SRM offers the following distinct advantages for modelling HCCI engines: First, it includes detailed chemical kinetics. Second, it accounts for the inhomogeneities in temperature and composition by a) including a coalescence-dispersion based turbulent micro-mixing sub-model to account for the mixing between burnt and unburnt species, and b) accounting for fluid-wall interactions and fluctuations, inherent to combustion engine operations.

From the HCCI commercialization perspective, controlling HCCI operation still remains a formidable challenge. Fuelling an HCCI engine with two different fuels with distinct auto-ignition characteristics (octane number) is a potential controlling parameter for HCCI operation. Olsson et al. (2000) operated an HCCI engine with port injected dual fuels (iso-octane and n-heptane) and obtained engine control by varying the octane number. Iso-octane was replaced by ethanol in their next investigation to exploit a higher octane number range (Olsson et al.; 2001). In that study, the dual fuelled HCCI engine was turbo-charged to enable operation at high load. In the absence of inlet air heating, the ratio of ethanol to n-heptane was the sole candidate for controlling combustion timing. Even at high load, NO_x emissions were observed to be low, thus proving the overall effectiveness of HCCI technology in producing low NO_x . Stanglmaier et al. (2001) performed measurements on a 6-cylinder turbo-charged dual fuelled engine to demonstrate the control of combustion phasing relative to the cycles. Improvement in fuel efficiency (10-15%) and ultra-low NO_x emissions were the features of running Fischer-Tropsch naphtha plus natural gas fuelled HCCI operation at low to moderate loads and conventional SI mode with natural gas fuel at high loads. They referred to this method of controlling combustion phasing as fuel-blending. Furthermore, the disadvantage pertaining to the on-board storage of the supplementary fuel and the commercial availability of the secondary fuel such as F-T naphtha, have also been pointed out. Ion current measurements were carried out to control a port injected, dual fuelled (ethanol and a 50-50 mixture of n-heptane and ethanol), HCCI engine (Strandh et al.; 2004). Closed loop control on a cycle-to-cycle basis was obtained with two methods, namely, an ion sensor and a pressure sensor. It was further demonstrated that the two methods gave a similar control performance. Recently, while defining the auto-ignition quality of fuels, Kalghatgi et al. (2003) have pointed out that the auto-ignition behaviour cannot be adequately explained in terms of a research octane number (RON) and a motor octane number (MON). RON and MON only describe the ignition quality of fuel at the RON and MON conditions. For other operating conditions, these cannot be used due to the sensitivity attached to the real fuels by the olefins, aromatics and oxygenates present in the fuel. Risberg et al. (2003) have used octane index,

OI to describe the ignition quality of fuels for HCCI engines. In the present work, the two fuels used are iso-octane and n-heptane for which RON and MON are equal and have been denoted as octane number (ON).

In this paper, we employ an integrated SRM based engine cycle simulator to investigate the factors for a reliable prediction of CO emissions, and the effect of octane number variation on HCCI combustion characteristics. Such an integrated approach combines the individual benefits of a full cycle simulator and the improved SRM. The paper is organized as follows: First, the experimental set up and the model are described. Then the model is validated by comparing the predicted combustion parameters and emissions with experimental results for a base case. On the basis of the model implemented, sources of CO emissions are identified. This is followed by the study involving the effect of implementing the stochastic convective heat loss sub-model on the in-cylinder temperature distribution. Finally, the engine cylinder wall temperature sensitivity and the effect of octane number variation on combustion parameters and emissions such as CO, HC and NO_x are presented.

2 Engine description

For the present work, a 6-cylinder SCANIA engine converted to run in HCCI mode was used for modelling. The engine parameters are given in Table 1. Olsson et al. (2000) performed the measurements on this engine. The engine had four valves per cylinder and the original injection system had been replaced by a low pressure sequential system for port injection of gasoline. For each of the two intake ports, one injector was installed; thus different fuel mixtures could be tested and individually adjusted for each cylinder. Iso-octane and n-heptane were the two fuels used. The engine inlet temperature was fixed by means of an electrical heater placed between the compressor and the inlet manifold.

Table 1: *Scania engine parameters.*

Description	Value
Displaced Volume	11705 cm ³
CR	18 : 1
Bore	126.6 mm
Stroke	154 mm
Connection Rod	255 mm
Exhaust Valve Open	96 ^o BBDC (at 1 mm lift)
Exhaust Valve Close	52 ^o ATDC (at 1 mm lift)
Inlet Valve Open	54 ^o BTDC (at 1 mm lift)
Inlet Valve Close	78 ^o ABDC (at 1 mm lift)

Following the description of the engine set-up, the PDF based full cycle simulator is explained in the next section.

3 Model description

The closed volume improved SRM was coupled with a 1-D finite difference code (GT-POWER) to form a PDF based engine cycle simulator.

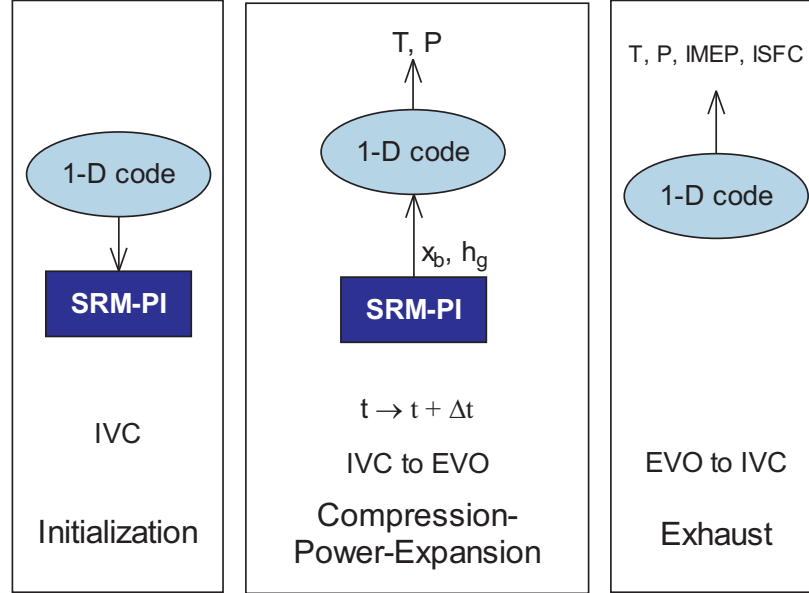


Figure 1: Coupling between the SRM and 1-D code.

A schematic of the coupling between the SRM and the 1-D code is shown in Figure 1. At IVC, the 1-D code provided the amount of internal EGR or residual burnt fraction (RBF), temperature and pressure to the SRM. Equipped with this information, the SRM simulated the compression, ignition and expansion strokes using a time splitting technique with time step, Δt . At each global time step, Δt , two variables namely, the convective heat transfer coefficient, h_g , and the cumulative burnt fraction, x_b , were used as progress variables and passed back to the 1-D code by the SRM. The SRM calculated the cumulative burnt fraction according to:

$$x_b = \frac{H_t - H_{tu}}{H_{tb} - H_{tu}} \quad (1)$$

where, H_{tu} and H_{tb} are the enthalpies of formation of the unburnt and burnt gases and H_t is the enthalpy of formation of the current mixture. Thus the SRM operates from IVC until exhaust valve opening (EVO). As shown in Figure 1, the CO, HC and NO_x emissions as well as the evolution of other chemical species were obtained

from the SRM. Whereas the in-cylinder pressure and temperature evolution, and the engine performance characteristics such as IMEP, BSFC were given by the 1-D CFD code.

The SRM is described as follows:

$$\begin{aligned} \frac{\partial}{\partial t} \mathcal{F}(\psi, t) + \frac{\partial}{\partial \psi_i} (G_i(\psi) \mathcal{F}(\psi, t)) - \frac{C_\phi}{2\tau} \iint K(\psi, \psi_p, \psi_q) \mathcal{F}(\psi_p) \mathcal{F}(\psi_q) d\psi_p d\psi_q \\ = \frac{-1}{h} \left[U(\psi_{S+1} + h) \mathcal{F}(\psi_1, \dots, \psi_S, \psi_{S+1} + h, t) - U(\psi_{S+1}) \mathcal{F}(\psi, t) \right] \end{aligned} \quad (2)$$

with the initial conditions:

$$\mathcal{F}(\psi, 0) = \mathcal{F}_0(\psi)$$

where, \mathcal{F} is the mass density function (MDF) of the scalars (mass fractions of species ψ_1, \dots, ψ_S and temperature ψ_{S+1}) represented by the vector ψ . The convective heat loss and the source term G_i are given as:

$$U = \frac{-h_g A}{c_v m} (T - T_w) \quad (3)$$

$$G_i = \frac{M_i}{\rho} \sum_{j=1}^r \nu_{i,j} \omega_j \quad i = 1, \dots, S \quad (4)$$

$$G_{S+1} = \frac{1}{c_v} \sum_{i=1}^S \left(h_i - \frac{RT}{M_i} \right) \frac{M_i}{\rho} \sum_{j=1}^r \nu_{i,j} \omega_j + \frac{P}{m c_v} \frac{dV}{dt} \quad (5)$$

where, A , T , and T_w denote the area, mean in-cylinder temperature and wall temperature respectively. Furthermore, ρ , ν , ω , M_i , m , and c_v stand for the density, stoichiometric coefficient, molar rate, species molecular weight, total mass, and the specific heat at constant volume respectively. Instantaneous volume V was calculated according to the slider crank formula and the pressure P was calculated using ideal gas law (Kraft et al.; 2000; Bhave et al.; 2004). A detailed chemical mechanism containing $S = 157$ species and $r = 1552$ reactions was used to simulate the ignition process (Cantore et al.; 2002). The third term on the L.H.S. of (2) represents the coalescence-dispersion mixing sub-model (Curl; 1963), where the kernel,

$$K(\psi, \psi_p, \psi_q) = \delta \left(\psi - \frac{1}{2}(\psi_p + \psi_q) \right).$$

The finite difference scheme on the R.H.S. of (2) denotes the effect of convective heat loss on the MDF where, ψ_{S+1} is the temperature variable and h stands for the fluctuation. A Monte Carlo method with a first order time splitting scheme was employed to solve (2). The method involved approximating the initial density with an equi-weighted stochastic particle ensemble. Then, these particles were moved according to the evolution of the density function. As an initial condition, the same mean temperature and composition at IVC was allocated to all the stochastic particles. That was followed by a time marching step of size $\Delta t = 0.3$ CAD, and performing mixing, reaction and heat loss events on the particle system.

At this point, the heat transfer and mixing events are explained. These events together account for a practical situation in an engine cylinder where a fluid particle can move to the wall and undergo convective heat transfer with respect to the colder cylinder wall, and during the piston movement mix with other particles in the bulk. The fluctuation h in (2) is represented in terms of the stochastic particle system as follows: $h^{(i)}$ of a particle i , is given as,

$$h^{(i)} = \frac{T^{(i)} - T_w}{C_h} \quad (6)$$

where $T^{(i)}$ is the stochastic particle temperature and C_h is the fluctuation constant, an input parameter calibrated during validation. C_h should be always greater than 1.0, in order to satisfy the Newton's law of cooling. Ideally, the information of this constant should be obtained from a multi-dimensional CFD code, which is the matter of future work. Thus, with the progress in time, depending on the temperature difference between the particle and the wall, and the values of h_g and C_h , a stochastic particle was chosen according to uniform distribution and was cooled or heated due to convection.

The mixing according to the coalescence dispersion model was performed by choosing two distinct stochastic particles according to uniform distribution and by assigning the mean of the scalar properties of these particles to each of the two particles. The turbulent mixing time used for the simulations was 0.02s Kraft et al. (2000). At each Δt , the cumulative burnt fraction and the convective heat transfer coefficient were passed from the SRM back to the 1-D code. Based on these progress variables, the 1-D code determined the evolution of the in-cylinder pressure, temperature and other engine performance parameters.

First, the flow inside the engine was initialized using the 1-D code alone until the pressure, temperature and mass flow rates were stabilized. Then the coupled cycles were started. At the first coupled cycle, no information about the composition of exhaust gas is available; therefore an external file was read specifying the gas composition. For the subsequent coupled cycles, the exhaust composition as evaluated by the SRM code was used to specify the internal EGR composition. Of the 6 inline cylinders, only for cylinder#1, the combustion was evaluated by means of the SRM code. For the remaining five cylinders, experimental cumulative burnt mass fraction profiles were provided.

4 Model validation

The PDF based engine cycle model was validated by comparing the predictions for the in-cylinder pressure, auto-ignition timing, as well as CO, HC and NO_x emissions with the measured values for a base case as described in Table 2.

For the parameters and conditions given in Table 1 and Table 2, the RBF estimated by the model, was found to be approximately 5-6% only. Thus during a coupled cycle

(SRM + 1-D code), at IVC the 1-D code passes the amount of RBF to the SRM. Based on this, the SRM code calculates the mass fractions of the species of the inlet mixture. A scheme of 14 uncoupled 1-D code cycles followed by 2 coupled cycles with 100 stochastic particles was considered sufficient to obtain a steady state solution. This scheme resulted in a computational time of 7 h on a 1GHz Pentium III PC. A constant of fluctuation $C_h = 20$ yielded the following prediction for combustion and emissions.

Table 2: Scania engine operating conditions for base case.

Description	Value
RPM	1500
Fuel	Iso-octane
λ	3.07
Octane number	100
Engine inlet temperature	424 K

Figure 2 presents the comparison between the in-cylinder pressure predicted by the SRM based and Homogeneous model based (Cantore et al.; 2002) full-cycle simulations with the experimental results (Olsson et al.; 2000).

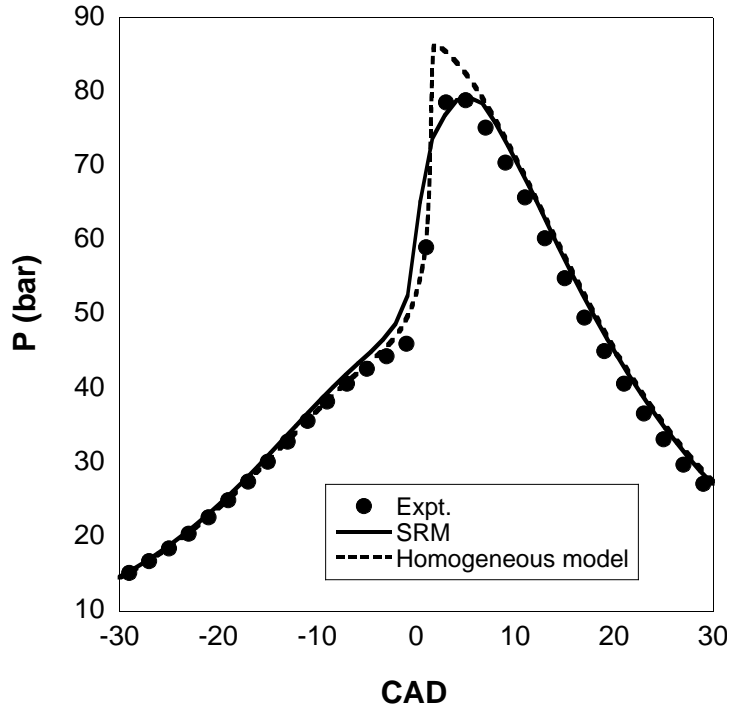


Figure 2: In-cylinder pressure profile (Homogeneous model, SRM and experiments).

The over-prediction in the peak pressure by the homogeneous model is due to its inability to account for the inhomogeneities in temperature and composition in the cylinder. For the same reason it also failed to predict the CO and HC emissions, however the ignition timing was correctly predicted by both the models, on account of the detailed chemistry.

Based on the pressure and emissions prediction, the SRM based full cycle model clearly outperformed the homogeneous model based engine cycle simulator. An excellent agreement between model predictions and experimental results was obtained for HC, CO as well as NO_x emissions (Fig. 3). Once calibrated during the base case, the value of the fluctuation constant $C_h = 20$ was kept constant throughout the paper.

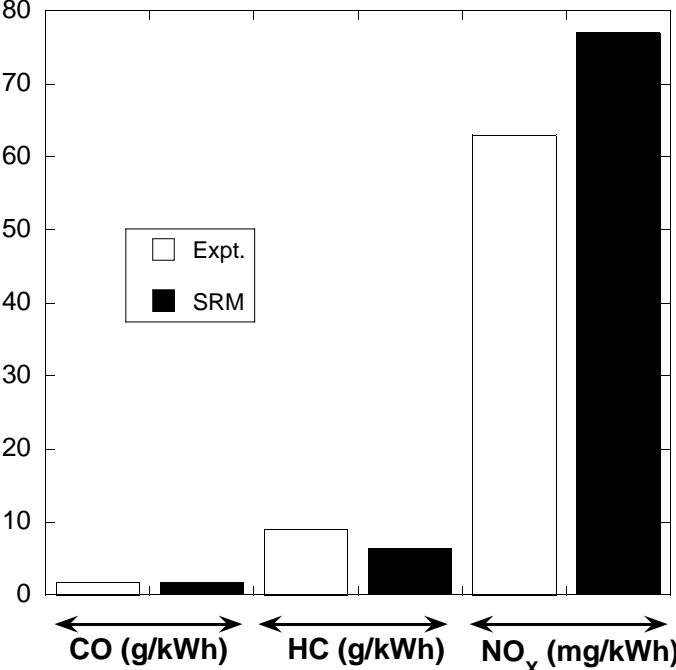
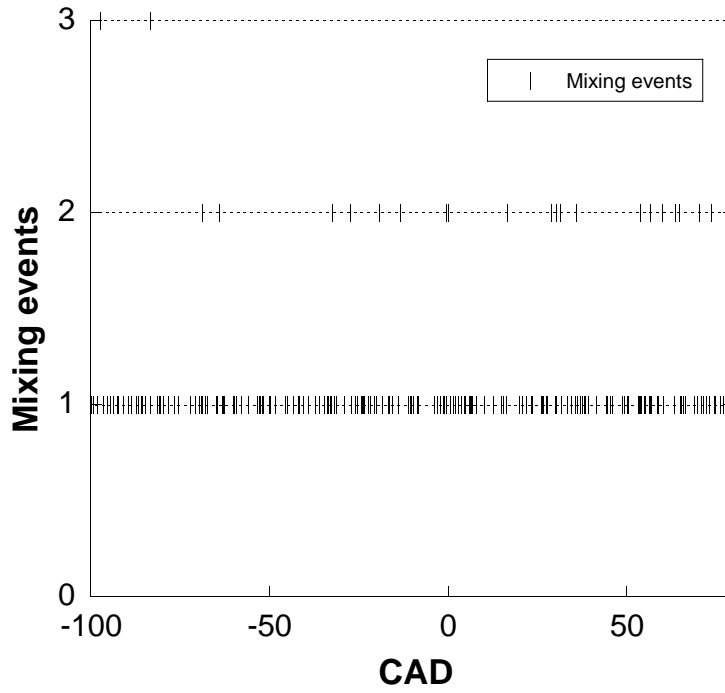
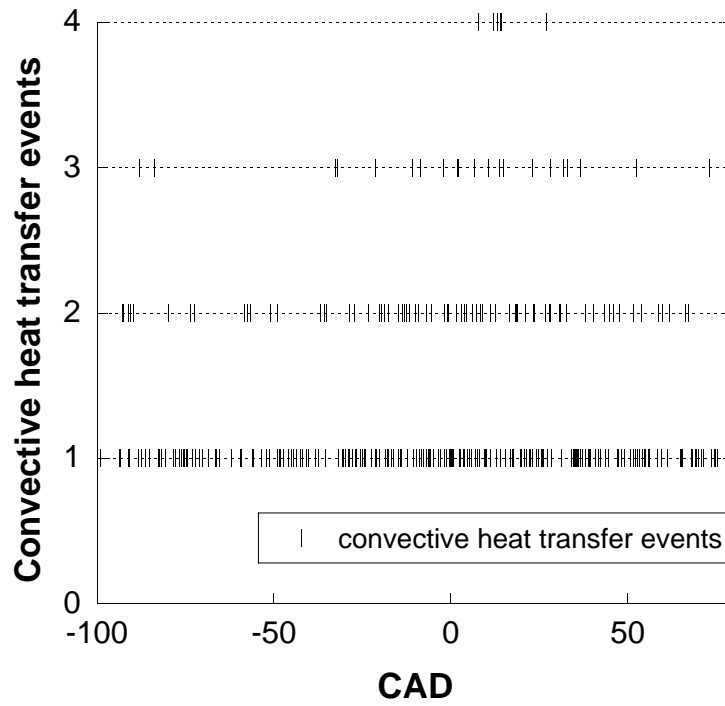


Figure 3: CO, HC and NO_x emissions: SRM prediction vs. measurements.

Thus, accounting for inhomogeneities in temperature and composition is crucial for reliably predicting the combustion parameters as well as the emissions. In the present model, the coalescence dispersion mixing and the stochastic convective heat transfer approaches account for these inhomogeneities. For the base case described above, the number of mixing and heat transfer events in a time step of size, $\Delta t = 0.3 \text{ CAD}$ are shown in Figure 4. For the given size of the time step, a maximum of four heat transfer events and three mixing events were observed to occur.



(a) Mixing events



(b) Convective heat transfer events

Figure 4: *Mixing and convective heat transfer events in the final coupled cycle.*

After the base case comparison, the validated model was used to understand the factors responsible for a reliable prediction of CO emissions.

5 CO emissions

The single-zone as well as multi-zone models face intrinsic difficulty in predicting the CO emissions. However, it has been pointed out in previous studies the rate constant for the CO oxidation reaction,



affects the CO prediction Ogink and Golovitchev (2002); Kong and Reitz (2003). The Arrhenius parameters for the reaction (7) are given in Table 3.

Table 3: Original (unchanged) Arrhenius parameters for CO oxidation.

Variable	Present work	Kong and Reitz (2003)
A (cc/mole/s)	6.0×10^6	1.51×10^7
β	1.5	1.3
E (cal/mol)	-740.9	-770

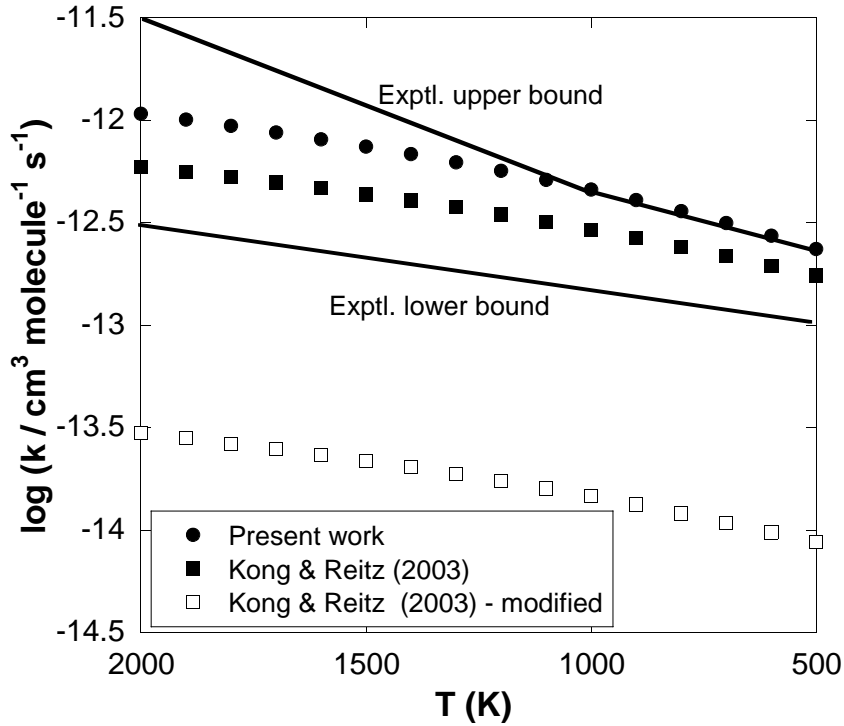


Figure 5: Comparison of the reaction rate constant as a function of temperature for CO oxidation reaction.

Figure 5 compares the rate constants as a function of temperature for the parameters presented in Table 3. The rate constant calculated with the Arrhenius parameters in the present work and that using the original Arrhenius parameters used by Kong and Reitz (2003) were within the band of the experimental scatter. The broad scatter in the experimental results for the rates of the reaction (7) at high temperature (500 to 2000 K) has been reported in the literature (Glassman; 1987). The upper and the lower bounds of the experimental data were taken from an exhaustive experimental data elsewhere (Baulch et al.; 1992).

In another study, assuming that a modification of the rate constant for the reaction (7) did not affect the auto-ignition characteristics, the rate constant for the reaction (7) was lowered to improve the CO emissions prediction (Ogink and Golovitchev; 2002). However, the modified Arrhenius parameters were not explicitly presented and hence were not used for comparison in the present work. Elsewhere, it was pointed out that lowering the value of pre-exponential constant A from 1.51×10^7 to 7.51×10^5 improved the CO prediction to 90% of the measured values (Kong and Reitz; 2003). The reaction rate constant with the modified Arrhenius parameters suggested a change of more than an order of magnitude and lies outside the band of measurements (Figure 5). In the present work, the rate constant of the CO oxidation reaction (7) has not been modified.

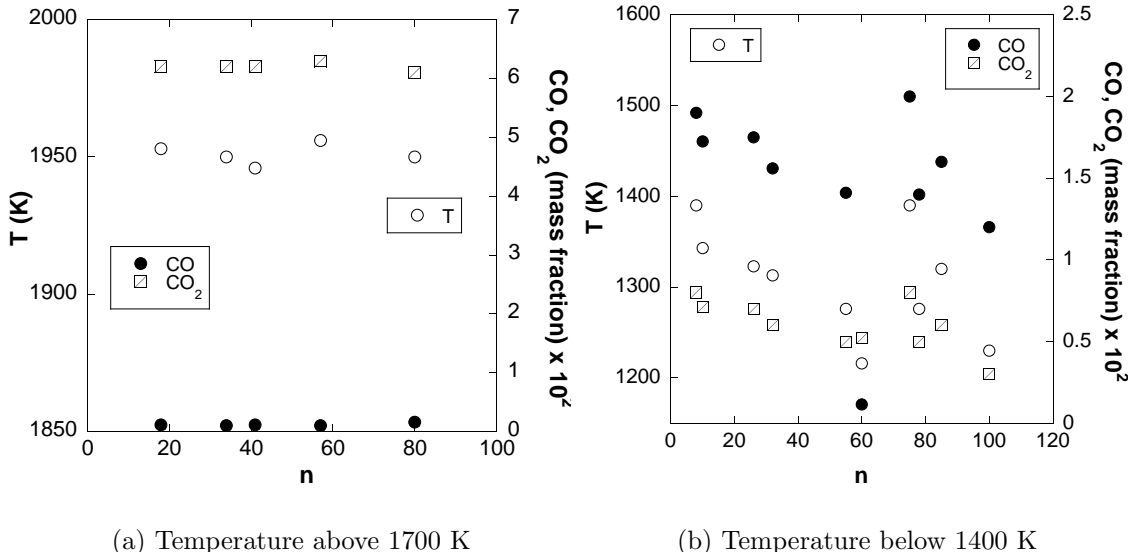


Figure 6: CO, CO₂ concentration and temperature of the stochastic particles.

The ignition crank angle degree for the validation base case was -0.2 CAD after top dead centre (ATDC). Figure 6(a) depicts the CO concentration and temperature of the stochastic particles with respect to the particle index, n , at 0.09 CAD ATDC. For the temperatures above 1700 K, the CO formed due to incomplete oxidation was converted to CO₂. Figure 6(b) denotes the particles from the ensemble which

were at a temperature lower than 1400 K. For such particles, the CO formed during auto-ignition, was trapped due to the temperature freezing, thus not contributing to any CO₂. Therefore the corresponding CO₂ mass fractions of the particles were an order of magnitude less than those obtained with high temperature particles (Fig. 6(a)).

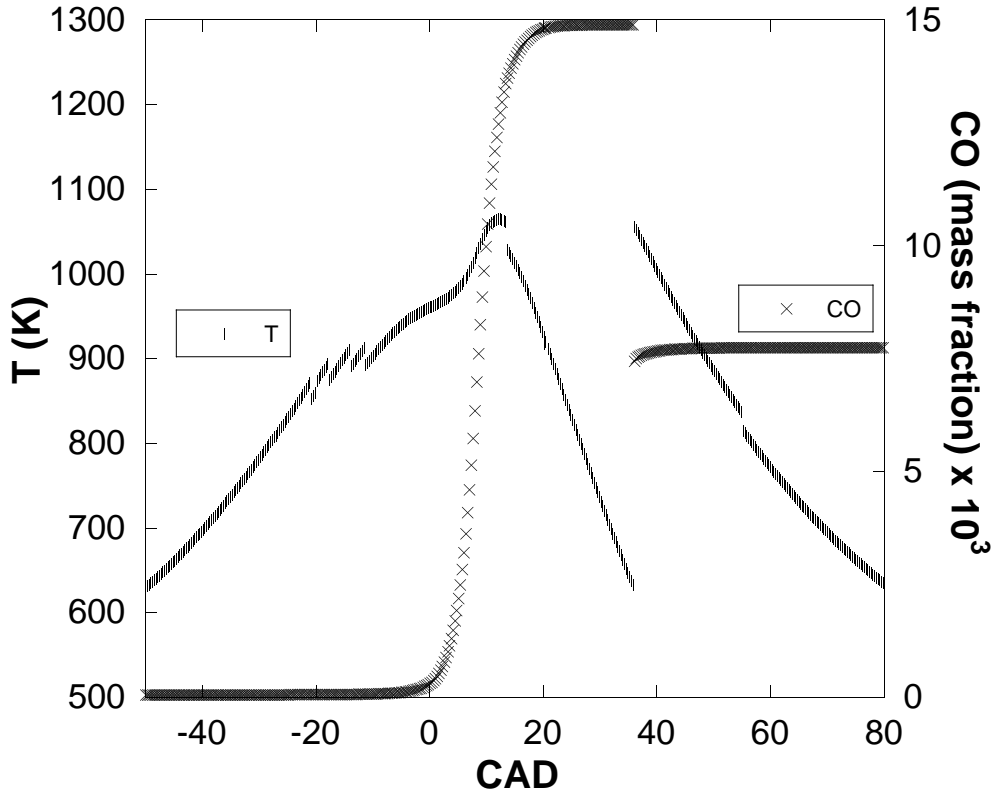


Figure 7: *CO mass fraction and temperature evolution of a stochastic particle.*

Next, we trace a single stochastic particle and study the evolution of its temperature and CO composition (Figure 7). For this, a particle from the ensemble was used to describe the effect of both mixing and convective heat loss on CO emissions. The mixing and heat transfer events with respect to the piston position are given in Table 4. From IVC until -20.2 CAD ATDC the temperature of the particle increased due to compression. Between -20.2 CAD and -11.6 CAD ATDC, the temperature of the particle reduced on account of one mixing and three convective heat loss events. Thus, the auto-ignition timing of a particle is sensitive to the fluctuations in temperature during the compression stroke. It should be noted that although the frequency of heat transfer and mixing events in a time step was quite high (Figure 4), the probability of selecting a single stochastic particle for heat transfer or mixing is low. At 7 CAD ATDC, the temperature of the particle increased due to ignition, resulting in the formation of CO. At 13.88 CAD ATDC, the particle experienced convective heat loss, and globally due to the expansion stroke, the temperature of

the particle reduced further. This reduction in temperature caused the freezing of the amount of CO mass fraction at a level of 15×10^{-3} .

Table 4: *Mixing and convective heat transfer events for a single stochastic particle.*

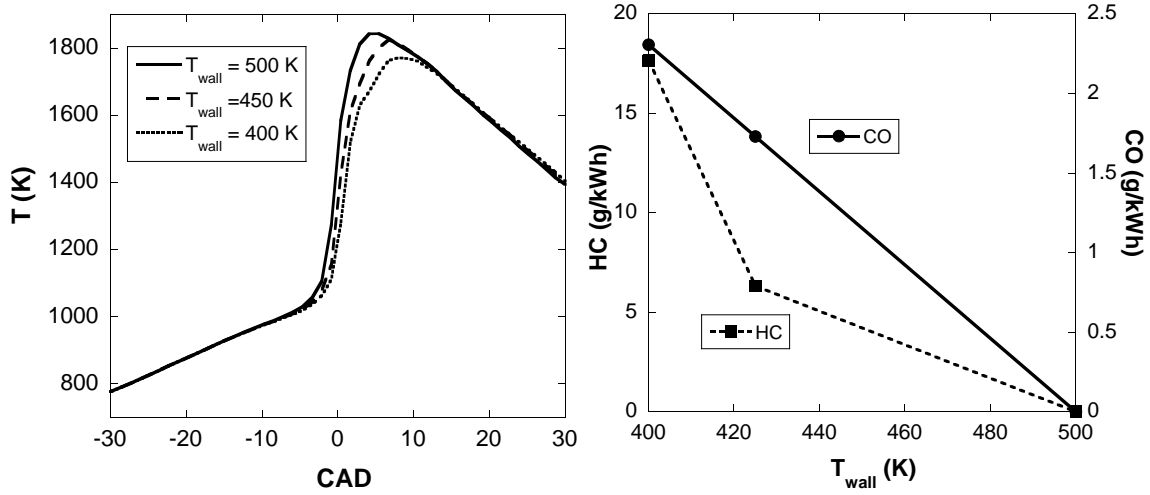
CAD (ATDC)	Event description
-21.08	convective heat transfer
-20.20	mixing
-17.99	convective heat transfer
-14.30	convective heat transfer
-11.60	convective heat transfer
13.88	convective heat transfer
36.80	mixing
55.50	convective heat transfer

At 36.8 CAD ATDC, the sudden rise in the temperature of the particle can be attributed to its mixing with a hotter particle of temperature, 1600 K. With such a high temperature, the hotter particle contained very low amount of CO. In consequence, at 36.8 CAD, the temperature of the particle surged to 1050 K, and the CO mass fraction dipped down to 7×10^{-3} . Following that the temperature of the particle continued to drop during expansion stroke and the CO mass fraction was frozen to a steady state.

Thus, the present work offers an explanation for the role of inhomogeneities due to mixing and convective heat loss, in the formation of CO emissions.

6 Wall temperature sensitivity

In the present work, the wall temperature was set to 450 K. However, the stochastic fluctuations are dependent on the temperature difference between the stochastic particles and the wall temperature. Thus, it is important to study the effect of change in wall temperature on the CO and unburnt HC emissions. For this, the model parameters as set in the base case validation were used and the wall temperature was varied as 400 K, 450 K and 500 K. Figure 8 depicts the effect of change in wall temperature on HCCI combustion and emissions. As expected, the increase in wall temperature raises the peak in-cylinder temperature (Figure 8(a)).



(a) In-cylinder temperature: sensitivity to wall temperature

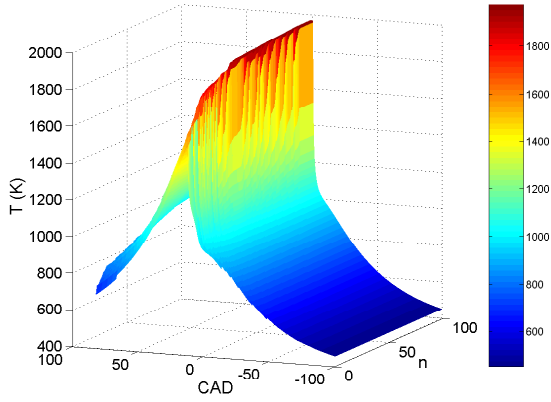
(b) CO, HC emissions: sensitivity to wall temperature

Figure 8: *Effect of variation in wall temperature.*

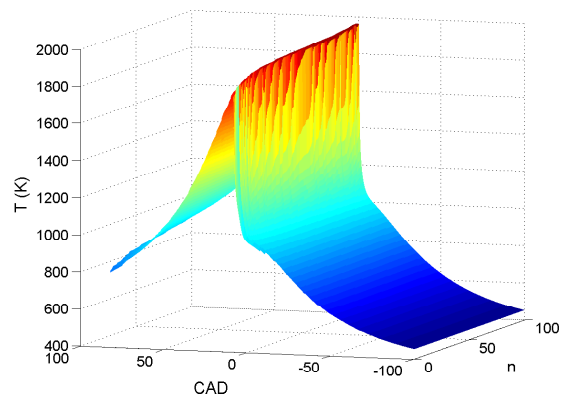
The CO and HC emissions are dependent on inhomogeneities induced due to the convective heat loss and turbulent mixing. For the wall temperature set at 500 K (Figure 8(b)) the air-fuel charge burnt almost completely, yielding extremely low CO and unburnt HCs in agreement with the results reported in the literature (Aceves et al.; 2001a). With a decrease of 50 K, CO and HC emissions resulted due to the incomplete oxidation. With a further 50 K drop in temperature CO emissions increased linearly along with a rise in HC emissions. The sensitivity of CO emissions to the wall temperature was observed to be more than that reported elsewhere (Kong and Reitz; 2003).

7 In-cylinder temperature distribution

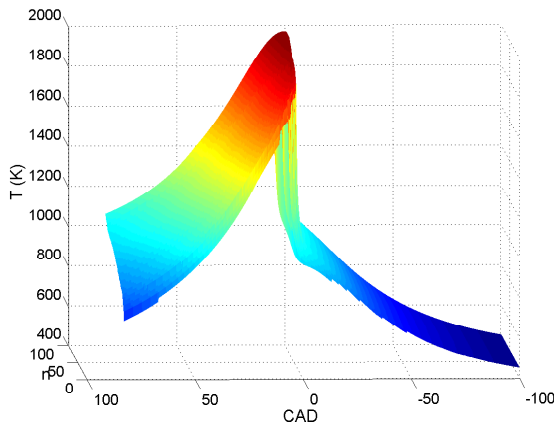
To investigate the effect of convective heat loss on the in-cylinder temperature distribution, the validated model was used with the base case conditions. Figure 9 depicts the in-cylinder temperature distribution with respect to the particle index, n , and crank angle degrees (CAD), for two values of the stochastic heat transfer parameter, $C_h = 20$ and $C_h = 60$. To show the effect of convective heat transfer alone, the mixing event was turned off and at the end of each global time step, the particles were sorted such that the lowest temperature was assigned to the first particle and the highest to the hundredth.



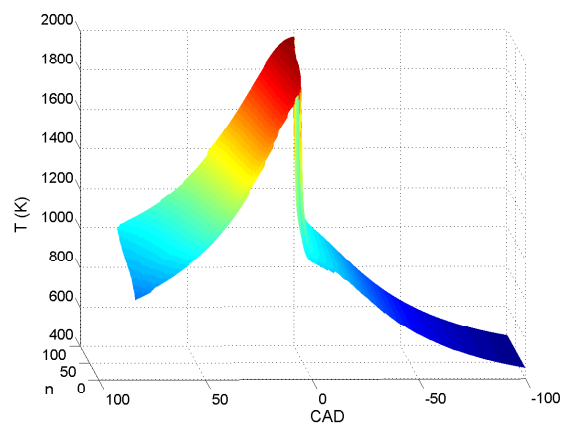
(a) $C_h = 20$, peak temperature



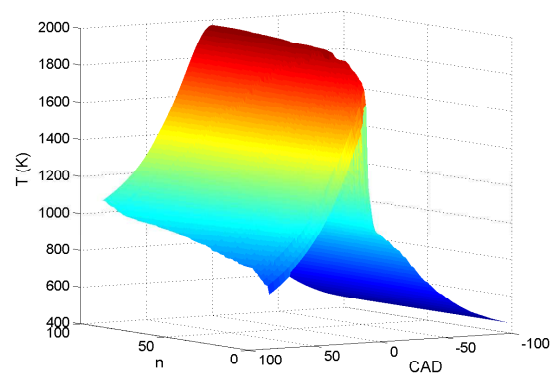
(b) $C_h = 60$, peak temperature



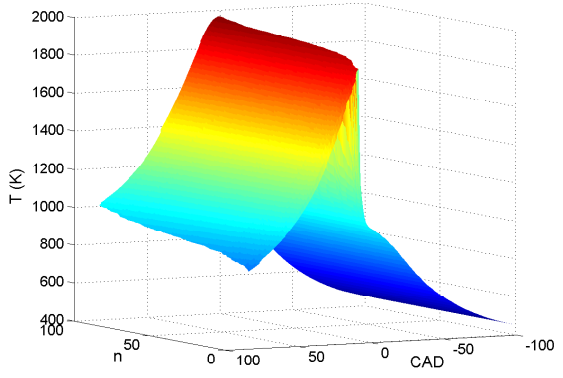
(c) $C_h = 20$, Auto-ignition timing



(d) $C_h = 60$, Auto-ignition timing



(e) $C_h = 20$, Particle temperatures at EVO



(f) $C_h = 60$, Particle temperatures at EVO

Figure 9: *Effect of variation in C_h .*

From Fig. 9(a) and Fig. 9(b) it can be observed that the particles in the range of approximately 40-100 burnt instantaneously for $C_h = 20$ thus having a very slight difference in peak temperatures, whereas relatively more particles (20-100) burnt spontaneously for $C_h = 60$. For $C_h = 20$, the magnitude of fluctuations is larger than that with $C_h = 60$, however the number of fluctuations is higher in the latter case. As depicted in Fig. 9(c) a scatter of temperature profiles for individual particles is obtained as a result of the inhomogeneity, in contrary to the almost spontaneous auto-ignition of the particles for the case, $C_h = 60$ (Fig. 9(d)). Even at EVO, the inhomogeneities continued to exist; the temperature difference between the coolest and the hottest stochastic particles for $C_h = 20$ being 400 K (Fig. 9(e)) and that for $C_h = 60$ being approximately 200 K (Fig. 9(f)). The inhomogeneities in the expansion stroke dictate the level of CO emissions obtained at the exhaust.

8 Octane number variation

Octane number (ON) is a practical measure of a fuel’s resistance to knocking and by definition it denotes the volume percentage of iso-octane in an iso-octane and n-heptane mixture. Iso-octane and n-heptane are widely different in their auto-ignition characteristics and this fact is used to control the HCCI combustion and emissions.

In this section the model predictions are compared with measurements for varying octane numbers. The number of particles, N , the cycles and the parameter C_h were kept the same as in the previous section. The operating conditions for this study are given in Table 5.

Table 5: Scania engine operating conditions for ON variation study.

Description	Value
RPM	1500
Fuels	Iso-octane and n-heptane
λ	3.72
Octane number	Varying
Engine inlet temperature	310 K
Engine inlet pressure	0.99 bar

With the engine speed fixed at 1500 rpm and the air-fuel ratio, λ , at 3.72, the octane number was varied from 61 to 86. Ignition CAD is the crank angle degree at which 10% of the air-fuel mixture burns. Figure 10(a) depicts the behaviour of the ignition-CAD as the octane number varies. With increasing octane number, the high temperature heat release is delayed, represented by the retarded ignition timing. Over this range of octane numbers, the predicted ignition-CAD lies reasonably

within the bounds of the experimental results. The combustion duration, i.e. the angle between 10% and 90% burned fraction is shown in Figure 10(b).

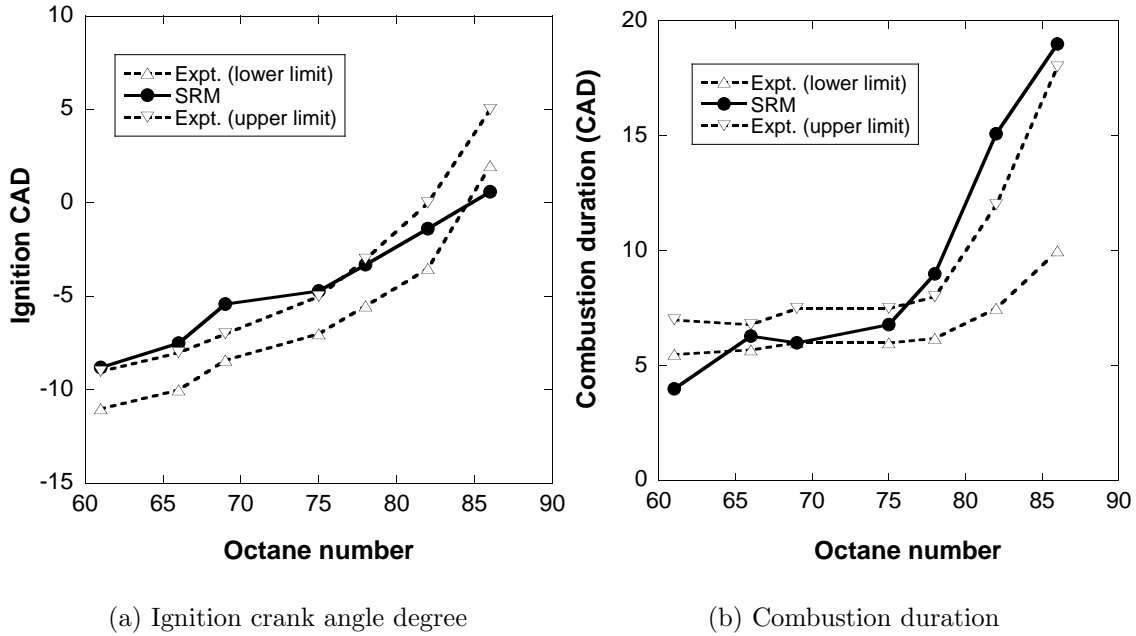


Figure 10: *Ignition characteristics.*

The experimental data and model predictions for CO, unburnt HC and NO_x emissions are plotted in Figure 11. With increasing octane number, the expected rise in CO and HC emissions due to incomplete oxidation was predicted correctly by the model. Overall, the trends as well as magnitudes are predicted well as compared to the experimental results. In particular at low octane numbers (61, 66 and 69), the CO and HC emissions are under-predicted by 80 % and 65 % respectively. Smaller combustion duration predicted in this range and the constant wall temperature used could be responsible for this discrepancy. The NO_x ($\text{NO} + \text{NO}_2$) emissions were observed to be low over the entire octane number range investigated. As shown in Fig. 11 the predicted NO_x emissions with varying octane number, showed a good agreement with the measurements.

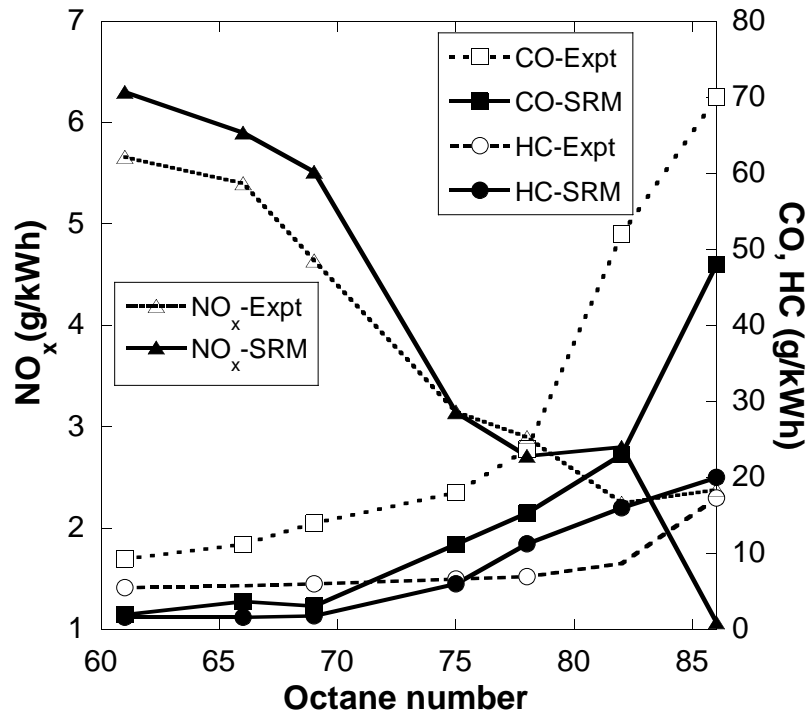


Figure 11: CO, HC and NO_x emissions: sensitivity to octane number.

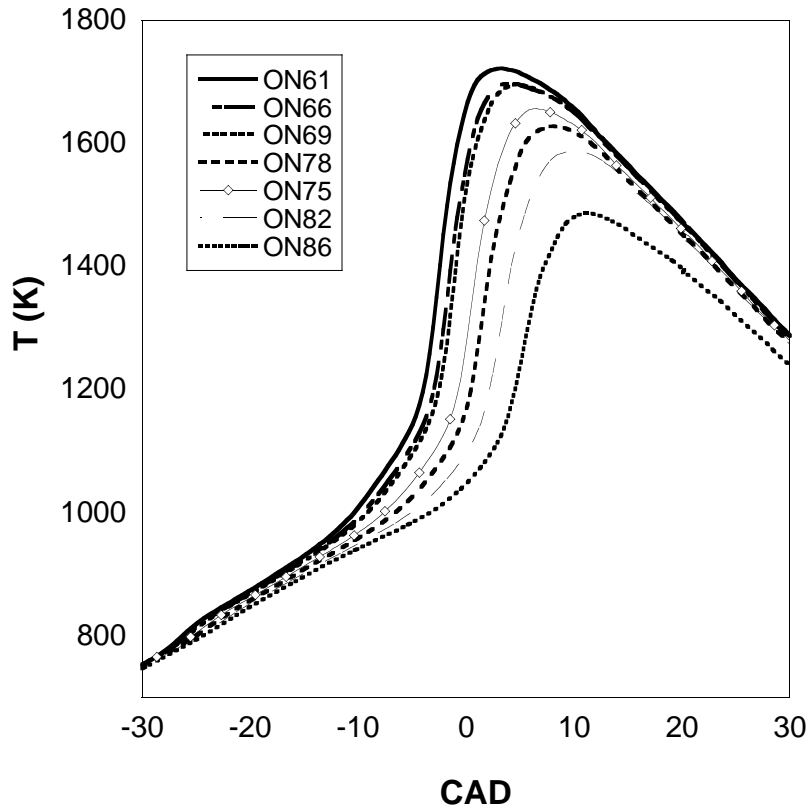


Figure 12: Effect of octane number variation on in-cylinder temperature.

Figure 12 shows the effect of octane number variation on the in-cylinder temperature. A decrease in the octane number (larger amount of n-heptane) activates the low temperature chemistry resulting in advanced auto-ignition. This incites the high temperature heat release leading to higher peak temperatures.

9 Conclusions

A dual fuelled homogeneous charge compression ignition (HCCI) engine was modelled using an integrated PDF-based engine cycle simulator.

The robustness and accuracy of the integrated model are evident from the excellent agreement observed between model predictions and measurements for in-cylinder pressure and CO, HC as well as NO_x emissions for the base case. The model outperformed the widely used homogeneous model-based full cycle simulators.

Furthermore, the importance of accounting for the inhomogeneities in accurately predicting CO emissions was demonstrated on the basis of a stochastic convective heat loss approach and coalescence-dispersion mixing. Prediction of CO emissions was identified to be most sensitive to three factors namely, fluid-wall interactions, mixing of the hot and cold fluid parcels, and the temperature of the cylinder wall. Particularly, the inhomogeneities occurring during compression stroke dictated the ignition timing of the stochastic particle, and hence the rate of formation of CO.

After the validation, the model was also applied to study the effect of change in octane number on combustion and emissions. With an increase in octane number, the retardation of the main stage heat release rate delayed the ignition timing and reduced the peak temperature. Increasing CO and HC emissions (incomplete oxidation) and the decrease in NO_x emissions with increasing octane number were correctly predicted and showed a reasonably good agreement with measurements.

10 Acknowledgements

Financial support from the Cambridge Commonwealth Trust and the Centre for Scientific Enterprise Ltd. are kindly acknowledged. The authors are thankful to Prof. B. Johansson at the Division of Heat and Power, Lund Institute of Technology, Sweden for providing the experimental data.

References

Aceves, S. M., Flowers, D. L., Martinez-Frias, J., Smith, J. R., Westbrook, C. K., Pitz, W. J., Dibble, R., Wright, J. F., Akinyemi, W. C. and Hessel, R. P. (2001a). A sequential fluid-mechanic chemical-kinetic model of propane hcci combustion, *SAE Paper 2001-01-1027*.

- Aceves, S. M., Flowers, D. L., Westbrook, C. K., , Smith, J. R., Pitz, W., Dibble, R., Christensen, M. and Johansson, B. (2000). A multi-zone model for prediction of hcci combustion and emissions, *SAE Paper 2000-01-0327*.
- Aceves, S. M., Martinez-Frias, J., Flowers, D. L., Smith, J. R., Dibble, R., Wright, J. F. and Hessel, R. P. (2001b). A decoupled model of detailed fluid mechanics followed by detailed chemical kinetics for prediction of iso-octane hcci combustion, *SAE Paper 2001-01-3612*.
- Baulch, D. L., Cobos, C. J., Cox, R. A., Esser, C., Frank, P., Just, T., Kerr, J. A., Pilling, M. J., Troe, J. W., W. R. and Warnatz, J. (1992). Evaluating kinetic data for combustion modeling, *J. Phys. Chem. Ref. Data* **21**: 411–569.
- Bhave, A. N., Balthasar, M., Mauss, F. and Kraft, M. (2004). Analysis of a natural gas fuelled hcci engine with exhaust gas recirculation using a stochastic reactor model, *Int. J. Engine Res.*
- Cantore, G., Montorsi, L., F., M., Amneus, P., Erlandsson, O., Johansson, B. and Morel, T. (2002). Analysis of a 6 cylinder turbocharged hcci engine using a detailed kinetic mechanism, *ASME Paper 2002-ICE-457*.
- Curl, R. L. (1963). Dispersed phase mixing: I. theory and effects in simple reactors, *A. I. Ch. E. Journal* **9**(2): 175–181.
- Easley, W. L., Agarwal, A. and Lavoie, G. A. (2001). Modeling of hcci combustion and emissions using detailed chemistry, *SAE Paper 2001-01-1029*.
- Fiveland, S. B. and Assanis, D. N. (2001). Development of a two-zone hcci combustion model accounting for boundary layer effects, *SAE Paper 2001-01-1028*.
- Flowers, D. L., Aceves, S. M., Martinez-Frias, J. and Dibble, R. W. (2002). Prediction of carbon monoxide and hydrocarbon emissions in iso-octane hcci engine combustion using a multizone model, *Proc. Comb. Inst.* **29**: 687–694.
- Glassman, I. (1987). *Combustion*, 2nd edn, Academic Press, New York, p. 66.
- Kalghatgi, G., Risberg, P. and Angstrom, H. E. (2003). A method of defining ignition quality of fuels in hcci engines, *SAE Paper 2003-01-1816*.
- Kong, S. C. and Reitz, R. D. (2003). Numerical study of premixed hcci engine combustion and its sensitivity to computational mesh and model uncertainties, *Combust. Theory Modelling* **7**: 417–433.
- Kraft, M., Maigaard, P., Mauss, F., Christensen, M. and Johansson, B. (2000). Investigation of combustion emissions in a homogeneous charge compression injection engine: Measurements and a new computational model, *Proc. Combust. Inst.* **28**: 1195–1201.

- Maigaard, P., Mauss, F. and Kraft, M. (2003). Homogeneous charge compression ignition engine: A simulation study on the effects of inhomogeneities, *J. Eng. Gas Turbines Power* **125**: 466–230.
- Ogink, R. and Golovitchev, V. (2002). Gasoline hcci modelling: An engine cycle simulation code with a multi-zone combustion model, *SAE Paper 2002-01-1745*.
- Olsson, J. O., Erlandsson, O. and Johansson, B. (2000). Experiments and simulation of a six-cylinder homogeneous charge compression ignition (hcci) engine, *SAE Paper 2000-01-2867*.
- Olsson, J. O., Tunestål, P., Haraldsson, G. and Johansson, B. (2001). A turbocharged dual fuel hcci engine, *SAE Paper 2001-01-1896*.
- Risberg, P., Kalghatgi, G. and Angstrom, H. E. (2003). Auto-ignition quality of gasoline-like fuels in hcci engines, *SAE Paper 2003-01-3215*.
- Stanglmaier, R. H., Ryan III, T. W. and Souder, J. S. (2001). Homogeneous charge compression ignition with a free piston: A new approach to ideal otto cycle performance, *SAE Paper 2001-01-1897*.
- Strandh, P., Bengtsson, J., Johansson, R., Tunestal, P. and Johansson, B. (2004). Cycle to cycle control of a dual-fuel hcci engine, *SAE Paper 2004-01-0941*.